Macromolecular Theory and Simulations
www.mts-journal.de

# The Presence of a Wall Enhances the Probability for Ring-Closing Metathesis: Insights from Classical Polymer Theory and Atomistic Simulations

*Ingo Tischler, Alexander Schlaich, and Christian Holm**

**The probability distribution of chain ends meeting when one end of the polymer is fixed to a certain distance to a reflecting wall is investigated. For an ideal polymer chain the probability distribution can be evaluated analytically via classic polymer theory. These analytical predictions are compared to atomistic MD simulations of one tethered alkane chain close to the wall. The results demonstrate that a confining wall can lead to a significant increase in the return probability for the chain ends, and thus, can increase the occurrence of ring-closing reactions. It is further demonstrated that the excess return probability shows a maximum at a certain distance, thereby yielding an optimal catalyst position in the ring-closing reaction.**

## 1. Introduction

Macrocyclization reactions[1–3] are a common tool for drug discovery and production in industry. Due to the bioactivity of macrocyclic molecules, they can be used as an antitumoral, antibiotics, or an antifungal. On the commercial side, they are often used as perfume components. One particular reaction is the ring-closing metathesis (RCM) of dienes.[4–6] As depicted in **Figure 1**, a competing pathway for this reaction is the oligomerization via the acyclic diene metathesis (ADMET), resulting in a so-called a ring-chain-equilibrium[7] that will diminish the efficiency of the RCM.

To increase the selectivity of ring-closing over polymerization, it is possible to decrease the concentration of the dienes, however, this is not feasible when trying to upscale the catalysis. In ref. [8] a novel biomimetic approach was suggested where the catalyst was brought into a cylindrical confining space, such that only very few (ideally one) substrates were able to enter the pore, resulting in preferential RCM and suppressed ADMET. Experiments of this metathesis in SBA-15 nano-tubes by Ziegler et al.[8] showed an increase in the selectivity due to confinement effects.

In this work, we investigate the impact of geometric confinement on the process of ring-closing of a single chain. To do so we assume that the probability of a ring-closing event is linearly related to the probability that the two ends of a chain are located within a center-to-center distance between zero and some reaction length $\lambda$. We start out by analyzing the end-to-end distance distribution for ideal Gaussian chains, and for molecular dynamic simulations of an atomistic representation of 18- and 28-monomer long alkane oligomers, where one of the end monomers is fixed in space, and located a distance $d$ away from a reflecting, that is, inert and impenetrable, surface. This set-up is motivated by the idea that a possible catalyst can be attached to a confining wall via molecular linker groups of various lengths at a certain distance. The comparison between the ideal chain and the atomistic oligomers is performed by mapping the oligomer conformational properties to an equivalent freely-jointed chain, whose statistical properties can be calculated analytically via classic polymer theory.[9] Previous analytic work on RCM for bulk systems has been done, for example, in refs. [10, 11]. Our analysis of this model suggests that the ring-closing probability of a tethered ideal chain is always enhanced compared to a free ideal chain, and that the two investigated united atom oligomers can show both an enhancement, and a diminishing, of the ring-closing probability, which depends on the tether distance $d$.

This article is organized as follows: First we describe the polymer theory and the notation for our set-up. In Section 3, we describe the investigated atomistic oligomer model, followed by the results in Section 4. We finish our article with the conclusions and outlook for further studies.

## 2. Theory

The theory of ideal Gaussian polymer chains (or classical random walks) is well understood,[9] and is summarized in the following section. Starting the random walk (RW) at the origin, a displacement of fixed length $b$, in one of the Cartesian directions is chosen randomly. Starting again from this point in space, the procedure is repeated $N$ times. If the probability to take a step in any direction is equally likely, the distribution of walks of a certain length (i.e., the end-to-end distance of the ideal polymer) is given by the binomial distribution. For long RWs, $N \gg 1$, the central limit theorem can be applied, and the

I. Tischler, Dr. A. Schlaich, Prof. C. Holm
Institute for Computational Physics
University of Stuttgart
70569 Stuttgart, Germany
E-mail: holm@icp.uni-stuttgart.de

The ORCID identification number(s) for the author(s) of this article can be found under https://doi.org/10.1002/mats.202000076.



**DOI: 10.1002/mats.202000076**

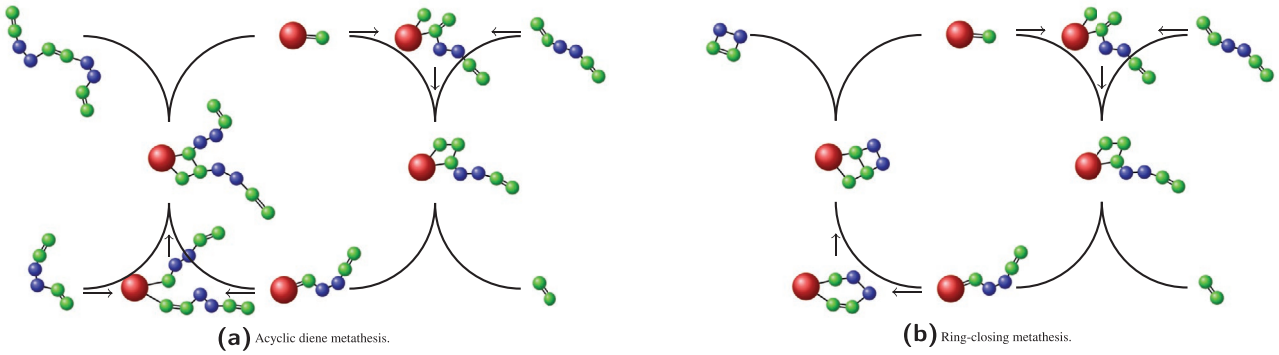


**Figure 1.** Scheme of different pathways for a diene metathesis reaction. The catalyst is shown in red, the green particles denote those carbon atoms that share a double bond. Only these can attach to the catalyst. The other backbone carbon atoms are depicted in blue. a) The different pathways of an acyclic diene metathesis is seen. A ring-closing metathesis is observed. In the center top, and center bottom stages, the catalyst can accept a bond from the green particles. In the center of the picture the bonds have been formed. The reaction can either continue forward, (clockwise) or backward (counter clockwise). This depends on the order with which the bonds will break. The right path for both reactions is the same up to the point where either (a) a carbon chain is attached to the catalyst, or (b) the two ends of the chain close onto themselves to form a ring.

probability of finding RWs with an end-to-end vector $\vec{x}$, can be approximated by a Gaussian of the form

$$P(\vec{x}) = \left(\frac{3}{2\pi R^2}\right)^{\frac{3}{2}} e^{\frac{-3\vec{x}^2}{2R^2}} \tag{1}$$

where we have introduced the length of the random walk, $R^2 = Nb^2$.

Considering all RWs which have the same end-to-end distance $R_e = |\vec{x}|$ from the origin we obtain the probability distribution $P_e(R_e)$ by integrating Equation (1) over the surface of a sphere of radius $R_e$.

$$P_e(R_e) = 4\pi R_e^2 \left(\frac{3}{2\pi R^2}\right)^{\frac{3}{2}} e^{\frac{-3R_e^2}{2R^2}} \tag{2}$$

To investigate interfacial and confinement effects on a random walk we introduce a reflecting wall at $z_w = -d$ (see **Figure 2**). A reflection occurs if in step $i$, a displacement is selected that would end in $z_i - z_w < 0$. In this case, the $z$-coordinate is mirrored at the wall such that $z_i = |z_i - z_w|$. While this approach does not conserve the step length $b$ upon a collision with the wall, it has the advantage of a well-defined inert, and impenetrable wall, without any additional degrees of freedom. The corresponding RW now starts a distance $d$ away from the surface, which corresponds to the distance of a stiff linker fixing polymer in space. The probability distribution function to find the other end of the polymer at position $\vec{x}$, is then given by[12]

$$P(\vec{x}, d) = \begin{cases} P(\vec{x}) + P(2d\,\hat{e}_z - \vec{x}) & z \geq -d \\ 0 & z < -d \end{cases} \tag{3}$$

Integration over the surface of a sphere of size $R_e$ to obtain the end-to-end distance yields

$$\begin{aligned} P_e(R_e, d) &= \frac{P_e(R_e)}{2}\left[\int_0^{\theta_e} \sin(\theta_e)\left(1 + e^{\frac{-6d(d+R_e\cos(\theta_e))}{R^2}}\right)\mathrm{d}\theta_e\right] \\ &= \frac{P_e(R_e)}{2}\left[1 - \cos(\theta_e) + \frac{R^2}{6dR_e}\left(e^{\frac{-6d(d+R_e\cos(\theta_e))}{R^2}} - e^{\frac{-6d(d+R_e)}{R^2}}\right)\right] \\ \text{with} \quad \theta_e &= \begin{cases} \pi & R_e \leq d \\ \pi - \arccos\left(\frac{d}{R_e}\right) & R_e > d \end{cases} \end{aligned} \tag{4}$$

which describes the end-to-end distribution of a random walk confined by a flat wall at distance $d$.

We now investigate the influence of the end-to-end probability distribution Equation (4) on the ring-closing probability. Whilst the latter depends on many variables including the local environment, diffusion, and transport of the substrate etc., here we assume that this scales linearly with polymer return probability $P_{pr}(d, \lambda)$. This assumption holds to leading order, as the ring-closing can only happen if the two polymer ends meet at least a characteristic distance $\lambda$ away from catalytic center, as indicated in Figure 2. The reaction radius $\lambda$ thus describes a sphere around the origin encapsulating the details of the catalytic reaction. The polymer return probability is correspondingly obtained by integrating the end-to-end distribution up to $\lambda$ by

$$P_{pr}(\lambda, d) = \int_0^{\lambda} P_e(R_e, d)\,\mathrm{d}R_e \tag{5}$$

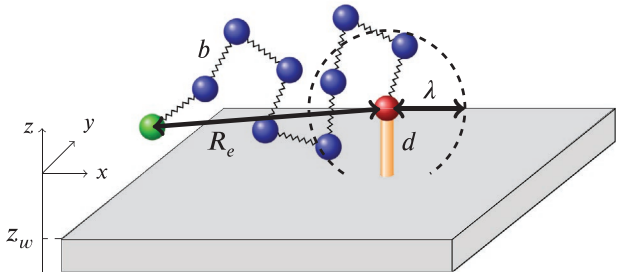


**Figure 2.** Illustration of the polymer model. One end of the chain (red) is held in place at a fixed linker length $d$. $R_e$ marks the end-to-end distance between the beginning and the end (green) of the chain. The dashed circle indicates the reaction radius $\lambda$ of the sphere over which Equation (5) is integrated.

It is instructive to compare the polymer return probability close to an interface to the case where the polymer is in bulk ("free" case, i.e., the polymer does not interact with the surface in the limit $d \to \infty$). To this end, we define the excess return probability due to the wall as

$$P_{\mathrm{ex}}(\lambda, d) = \frac{P_{\mathrm{pr}}(\lambda, d)}{P_{\mathrm{pr}}(\lambda, \infty)} - 1 \tag{6}$$

Equation (6) directly yields the increase in return probability—which we assume to be proportional to the selectivity increase — for an ideal polymer attached to a surface at a linker distance $d$.

To connect the ideal polymers that underlie a RW to chemically realistic alkane chains below, we rescale all lengths in our model by the Kuhn length defined as:[9]

$$b = \frac{\left\langle R_{\mathrm{e}}^2 \right\rangle}{R_{\max}} = \frac{\left\langle R_{\mathrm{e}}^2 \right\rangle}{(n-1) l \cos\left(\frac{\theta}{2}\right)} \tag{7}$$

Here, $R_{\max}$ is the maximal end-to-end distance of the polymer in equilibrium, $n$ is the number of monomers, $l$ is the bond length, and $\theta$ is the bond angle of the chemically realistic chains. This allows the mapping of the end-to-end distance to an equivalent freely jointed chain of segment length $b$, with the corresponding number of Kuhn segments

$$N = \frac{R_{\max}}{b} \tag{8}$$

Using such a mapping, any polymer will display the same average and-to-end distance as a RW, in the limit of long polymers.

## 3. Polymer Simulation

We model *n*-alkane chains using a chemically realistic united atom force field, with potential energy functions summarized in **Table 1**. The solvent was treated implicitly via Langevin dynamics with the Verlet integration scheme. To match the diffusion coefficient of methane, we chose a friction coefficient of $\gamma = 2.566/k_{\mathrm{B}}T$. We set the temperature to $T = 300$K, and the timestep to $\Delta t = 8$ fs. The total time over which each simulation was sampled was $t = 160$ µs. In analogy to the experiments performed by Ziegler et al.,[8] simulations for two sets of chain lengths $n \in \{18, 28\}$ were performed using the ESPResSo software package.[14]

In line with the theoretical considerations above we get rid of additional simulation parameters by employing a purely reflective wall. Particle positions which, after a position update are within the wall, are reflected according to $z_i = |z_i - z_{\mathrm{w}}|$, and their velocities in $z$-direction are reversed. The position of the $n = 1$ monomer was fixed at a distance $d$ from the reflecting wall and the end-to-end distance distribution was sampled for $d \in [0\text{Å}, 19\text{Å}]$. The sampling resolution was $\Delta d = 0.25$Å for $4\text{Å} < d < 14\text{Å}$, and $\Delta d = 1$Å in all other cases.

**Table 1.** United atom force field parameters taken from ref. [13]. The Lennard–Jones interactions have only been accounted for if between the two particles of the chain, there are at least three other particles (1–4 exclusion).

Pair bond potential

$$E(r) = \frac{k_r}{2}(r - r_0)^2$$

| Pair | $r_0$ [Å] | $k$ [kcal mol$^{-1}$/Å$^2$] |
|---|---|---|
| $CH_2$— $CH_2$ | 1.53 | 899 |
| $CH_2$— $CH_3$ | 1.53 | 899 |

Angle bond potential

$$E(\theta) = \frac{k_\theta}{2}(\theta - \theta_0)^2$$

| Pair | $\theta_0$ [°] | $k_\theta$ [kcal mol$^{-1}$/rad$^2$] |
|---|---|---|
| $CH_2$— $CH_2$— $CH_2$ | 112 | 120 |
| $CH_2$— $CH_2$— $CH_3$ | 112 | 120 |

Dihedral bond potential

$$E(\phi) = \frac{1}{2}[k_\phi^1(1 - \cos(\phi)) + k_\phi^2(1 - \cos(2\phi)) + k_\phi^3(1 - \cos(3\phi))]$$

| Pair | $k_\phi^1$ [kcal mol$^{-1}$] | $k_\phi^2$ [kcal mol$^{-1}$] | $k_\phi^3$ [kcal mol$^{-1}$] |
|---|---|---|---|
| $CH_2$— $CH_2$— $CH_2$— $CH_2$ | 1.6 | –0.8 | 3.24 |
| $CH_2$— $CH_2$— $CH_2$— $CH_3$ | 1.6 | –0.8 | 3.24 |

LJ-parameters

$$E(r) = 4\varepsilon\left[\left(\frac{\sigma}{r}\right)^{12} - \left(\frac{\sigma}{r}\right)^{6}\right]$$

| Pair | $\sigma$ [Å] | ε [kcal mol$^{-1}$] |
|---|---|---|
| $CH_2 \cdots CH_2$ | 4.009 | 0.09344 |
| $CH_2 \cdots CH_3$ | 4.009 | 0.14546 |
| $CH_3 \cdots CH_3$ | 4.009 | 0.22644 |

## 4. Results

The resulting end-to-end distance probability distribution from Equation (4), and the united atom MD simulations, are found in **Figure 3**. For the random walk theory one can easily proof that the random walk case for $d/b = 0$, that is, the random walk starts on the wall, is equal to the end-to-end distance probability distribution of an unconfined (free) random walk. This is due to symmetry reasons.

Moving the starting location slightly away from the wall results in a shift toward smaller end-to-end distances. If one increases the distance $d$ to values of about the average end-to-end distance of the free random walk, the end-to-end distance starts to approach the free case again. This time, however, the peak of the distribution gets larger, while the longer end-to-end distances appear less frequently. For even larger values of $d$, the peak shifts back to larger end-to-end distances, where again $P_{\mathrm{e}}$ lies above the free RW. For even larger values of $d$, the distribution will converge to that of a free random walk which is clear as the effects of the wall are rarely noticed by the monomers.

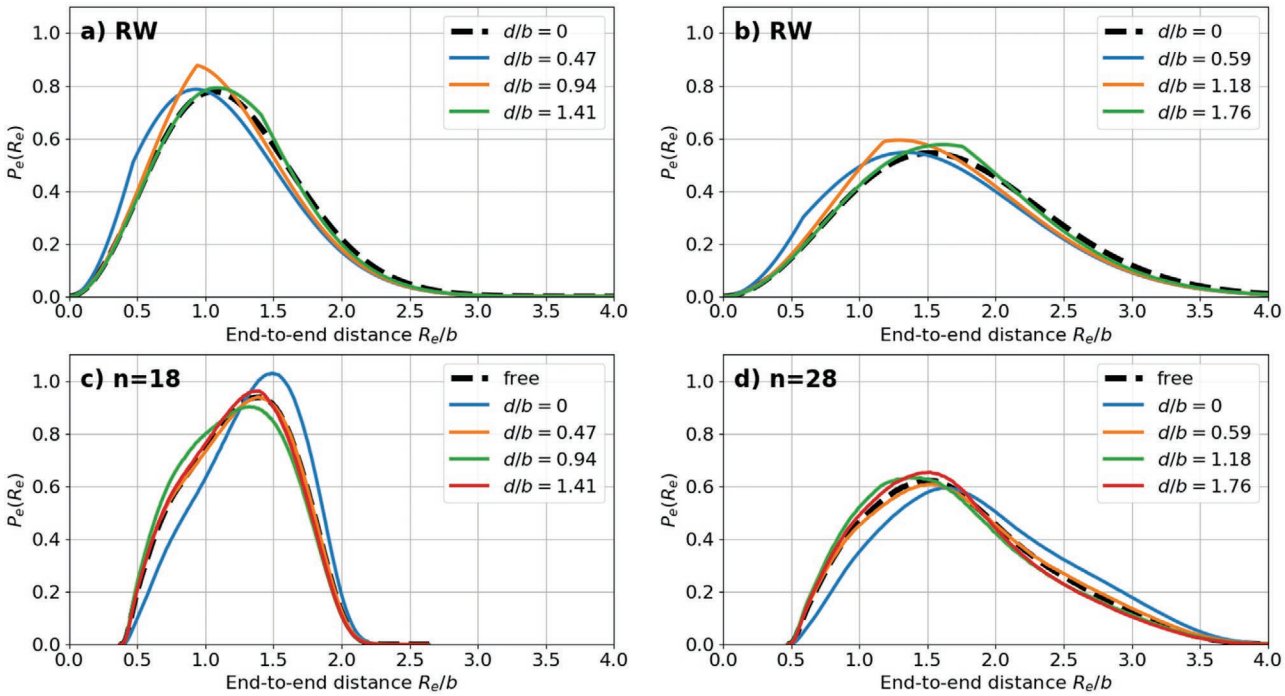


**Figure 3.** End-to-end probability distributions obtained via random walk theory (top) using Equation (4) and simulations (bottom) for the polymer chain lengths 18 (left) and 28 (right). The theoretical model used the Kuhn length $b$, and corresponding Kuhn segments $N$, calculated from the simulation data (Equations (7) and (8)). For the shorter chain these parameters are $b_{18} = 8.5$Å, and $N_{18} = 1.71$. For the longer chain, they are $b_{28} = 6.8$Å and $N_{28} = 3.49$.

This behavior can be observed for both chain lengths. The main difference is the observation that the longer chain prefers longer end-to-end distances.

From our simulations using the united atom model, we observe that the $n = 18$ chain for $d/b = 0$ varies strongly from the $n = 28$ chain. In both cases, it is important to note that the particle is practically embedded in the wall, and the chain starting from that point can only extend in the direction away from the boundary. Therefore, excluded volume effects contribute significantly to the end-to-end distribution, and correspondingly, $P_e(R_e)$ is shifted to larger end-to-end distances. For longer chain lengths, and large distances, the excluded volume effects become less important, and the distribution functions approach the analytical solution for the RW (see **Figure 4**b,d). Notably, at a certain distance $d$, the distribution functions for realistic polymer chains prefer to favor shorter end-to-end distances when compared to the RW. The simulation of chain length $n = 28$ is long enough to behave as predicted from a RW model, with the exception of the excluded volume at short end-to-end distances. The shorter chain, however, does not fit the model, and tends toward larger end-to-end distances.

Investigating the excess return probability (Figure 4), we observe a maximum in all 4 cases considered. For the analytical solution, we observe a dependency on the reaction radius $\lambda$, which is not present in the simulation data. This reaction radius, however, is not of experimental significance, as it corresponds to details of the reaction. The maximum itself on the other hand, tells us that we can have a significant increase in the polymer return probability, which further translates into a boost of the ring-closing probability. For our simulation we therefore would have expanded the ring-closing probability by 18.5%, given the optimal distance to the wall.

As can be observed from our simulation results in Figure 4c,d, the simulation show a range where the excess return probability is negative. This is both due to the excluded volume of the LJ-particles, which repel each other, and the stiffness of the polymer, and thus is expected to also correspond to real polymers anchored close to a wall.

## 5. Conclusion

We have investigated how the probability distribution of end-to-end distances for a single polymer chain changes when one end of the polymer is fixed at a certain distance from a reflecting wall. For an ideal Gaussian chain, this can be done analytically via classical polymer theory. By assuming that the ring-closing probability is linearly related to both polymer ends finding each other within a certain reaction radius $\lambda$, we have investigated the excess return probability, which reveals the corresponding change in the ring-closing probability due to the wall constraint. The theory of classical random walks yields a non-monotonic excess return probability that is always positive, and that displays a chain length dependent maximum, that varies monotonically with $d$. Since the Gaussian chain lacks any molecular interactions, we also performed the same investigations by performing molecular dynamics simulations of a united atom alkane model. The comparison with the random walk model was performed

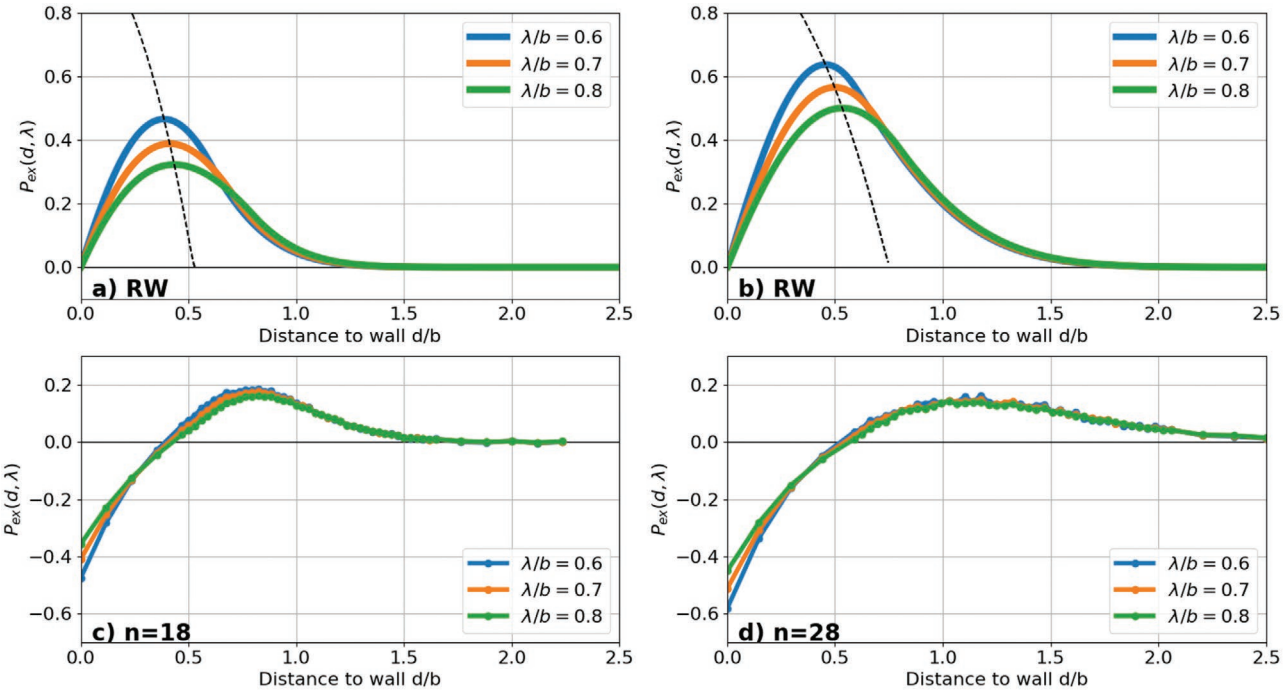


**Figure 4.** Excess return probability as defined in Equation (6). In the top row plots, a,b) we plot $P_e$ of the analytical RW solution, for three values of $\lambda/b$, calculated via the corresponding parameters of the equivalent freely jointed chain. The dotted line indicates the position of maxima for other values of $\lambda/b$. In the bottom plots, c,d) we display the corresponding $P_e$ of the simulation results for the united atom alkane chains with $n$ monomers.

by mapping the conformational properties of the united atom model, onto that of an equivalent freely jointed chain. For both, theory and simulation, we found an optimum in the excess return probability, which demonstrates a linker-length which maximizes the ring-closing probability. For the simulation of a polymer with $n = 18$ monomer units, we could measure an increase of up to 18.5% in comparison to a free polymer chain, whereas for the $n = 28$ chain, the increase was reduced to about 14.5%, albeit with a broader maximum. The optimal distances for the spacer length were for both cases about 7 Å, although the distribution is much broader for the longer chain. Interestingly, the ring-closing probability depended only weakly on $\lambda$ for the interacting chain simulations.

The advantage of single chain simulations is that they run very fast and allow for an easy change of the confining geometry and chain parameters. In the future we plan to perform multi-chain particle based simulations, in order to further study the influence of more complicated confining geometries on the selectivity of the RCM of dienes.

## Acknowledgements

This work was funded by the German Research Foundation (DFG) via Project-ID 358283783 – SFB 1333.

Open access funding enabled and organized by Projekt DEAL.

## Conflict of Interest

The authors declare no conflict of interest.

## Keywords

confinement, Gaussian chain statistics, MD simulations, polymer theory, random walk, ring-closing metathesis

Received: October 12, 2020
Published online:

[1] E. Marsault, M. L. Peterson, *J. Med. Chem.* **2011**, *54*, 1961.
[2] V. Marti-Centelles, M. D. Pandey, M. I. Burguete, S. V. Luis, *Chem. Rev.* **2015**, *115*, 8736.
[3] P. Ermert, *CHIMIA* **2017**, *71*, 678.
[4] R. H. Grubbs, *Tetrahedron* **2004**, *60*, 7117.
[5] A. Sytniczuk, M. Dąbrowski, Ł. Banach, M. Urban, S. Czarnocka-Śniadała, M. Milewski, A. Kajetanowicz, K. Grela, *J. Am. Chem. Soc.* **2018**, *140*, 8895.
[6] S. S. Kinderman, J. H. van Maarseveen, H. E. Schoemaker, H. Hiemstra, F. P. J. T. Rutjes, *Org. Lett.* **2001**, *3*, 2045.
[7] S. Monfette, D. E. Fogg, *Chem. Rev.* **2009**, *109*, 3783.
[8] F. Ziegler, J. Teske, I. Elser, M. Dyballa, W. Frey, H. Kraus, N. Hansen, J. Rybka, U. Tallarek, M. R. Buchmeiser, *J. Am. Chem. Soc.* **2019**, *141*, 19014.
[9] M. Rubinstein, R. H. Colby, *Polymer Physics*, Oxford University Press, Oxford **2003**.
[10] H. Jacobson, C. O. Beckmann, W. H. Stockmayer, *J. Chem. Phys.* **1950**, *18*, 1607.
[11] P. J. Flory, U. W. Suter, M. Mutter, *J. Am. Chem. Soc.* **1976**, *98*, 5733.
[12] S. Chandrasekhar, *Rev. Mod. Phys.* **1943**, *15*, 1.
[13] K. Bolton, Bosio, W. L. Hase, W. F. Schneider, K. C. Hass, *J. Phys. Chem. B* **1999**, *103*, 3885.
[14] F. Weik, R. Weeber, K. Szuttor, K. Breitsprecher, J. de Graaf, M. Kuron, J. Landsgesell, H. Menke, D. Sean, C. Holm, *Eur. Phys. J. Spec. Top.* **2019**, *227*, 1789.